Formation and growth of atmospheric nanoparticles in the eastern Mediterranean: Results from long-term measurements and process simulations

Nikos Kalivitis[1,2], Veli-Matti Kerminen[3], Giorgos Kouvarakis[1], Iasonas Stavroulas[1,4], Evaggelia Tzitzikalaki[1], Panayiotis Kalkavouras [1,5], Nikolaos Daskalakis[1,6], Stelios Myriokefalitakis[5,7], Aikaterini Bougiatioti[5], Hanna Elina Manninen[8], Pontus Roldin[9], Tuukka Petäjä[3], Michael Boy[3], Markku Kulmala[3], Maria Kanakidou[1], and Nikolaos Mihalopoulos[1,5]

1. Environmental Chemical Processes Laboratory, Chemistry Department, University of Crete, 70013, Heraklion, Greece

2. Institute for Astronomy, Astrophysics, Space Applications and Remote Sensing, National Observatory of Athens, I. Metaxa & Vas. Pavlou, 15236 Palea Penteli, Greece

3. Institute for Atmospheric and Earth System Research, Gustaf Hällströmin katu 2, P.O. Box 64, FI-00014 University of Helsinki

4. Energy, Environment and Water Research Center, The Cyprus Institute, Nicosia 2121, Cyprus

5. Institute for Environmental Research & Sustainable Development, National Observatory of Athens, I. Metaxa & Vas. Pavlou, 15236 Palea Penteli, Greece

6. Laboratory for Modeling and Observation of the Earth System (LAMOS), Institute of Environmental Physics (IUP), University of Bremen, Bremen, Germany,

7. Institute for Marine and Atmospheric Research (IMAU): Utrecht, Netherlands

8. Experimental Physics Department, CERN, 1211 Geneva, Switzerland

9. Lund University

Correspondence to: N. Kalivitis (nkalivitis@uoc.gr) and N. Mihalopoulos (nmihalo@noa.gr)

1 Abstract

2 Atmospheric New Particle Formation (NPF) is a common phenomenon all over the world. In
3 this study we present the longest time series of NPF records in the eastern Mediterranean
4 region by analyzing ten years of aerosol number size distribution data obtained with a mobility
5 particle sizer. The measurements were performed at the Finokalia environmental research
6 station on Crete, Greece during the period June 2008-June 2018. We found that NPF took
7 place 27% of the available days, undefined days were 23% and non-event days 50%. NPF is
8 more frequent in April and May probably due to the terrestrial biogenic activity and is less
9 frequent in August. Throughout the period under study, nucleation was observed also during
10 the night. Nucleation mode particles had the highest concentration in winter and early spring,
11 mainly because of the minimum sinks, and their average contribution to the total particle
12 number concentration was 8%. Nucleation mode particle concentrations were low outside
13 periods of active NPF and growth, so there are hardly any other local sources of sub-25 nm
14 particles. Additional atmospheric ion size distribution data simultaneously collected for more
15 than two years period were also analyzed. Classification of NPF events based on ion
16 spectrometer measurements differed from the corresponding classification based on a
17 mobility spectrometer, possibly indicating a different representation of local and regional NPF
18 events between these two measurement data sets. We used the MALTE-box model for
19 simulating a case study of NPF in the eastern Mediterranean region. Monoterpenes
20 contributing to NPF can explain a large fraction of the observed NPF events according to our
21 model simulations. However the adjusted parameterization resulting from our sensitivity tests
22 was significantly different from the initial one that had been determined for the boreal
23 environment.

24 1) Introduction

25 Most of the atmospheric aerosol particles, and a substantial fraction of particles able to act as
26 cloud condensation nuclei (CCN), have been estimated to originate from new particle
27 formation (NPF) taking place in the atmosphere (Spracklen et al. 2006; Kerminen et al., 2012;
28 Gordon et al., 2017). The exact mechanisms driving atmospheric NPF and subsequent particle
29 growth processes are still not fully understood, nor are the roles of different vapors and ions
30 in these processes (Kulmala et al., 2014; Lehtipalo et al., 2016; Tröstl et al., 2016). In order to
31 understand how aerosol particles affect regional and global climate and air quality, it is
32 necessary to quantify the factors that determine the occurrence of NPF and characterize the

parameters that describe the strength of NPF, such as the new particle formation and growth rates, in various environments.

While NPF has been reported to take place worldwide (Kulmala et al., 2004a; Wang et al., 2017), observational studies on this subject are scarce in rural sub-tropical environments. It has been shown that the processes responsible for particle formation and growth differ substantially across the European continent (Dall' Osto et al., 2018).

Several studies have investigated NPF in eastern Mediterranean and found it to be a frequent phenomenon. Lazaridis et al. (2006) first reported NPF at the area and correlated these events to polluted air masses. Petäjä et al. (2007) presented NPF in Athens metropolitan area and showed that under the influence of urban pollution, condensing species leading to growth of the new particles are far more hygroscopic than under cleaner conditions. NPF events have also been reported to be frequent at the urban environment of Thessaloniki (Siakavaras et al., 2016). Kalivitis et al. (2008) showed that precursors and nucleation mode particles experience strong scavenging on Crete island during summer. Pikridas at al. (2012) suggested that nucleation events occurred only when accumulation mode particles were neutral, being consistent with the hypothesis that a lack of NH_3, during periods when particles are acidic, may limit nucleation in sulfate-rich environments such as the eastern Mediterranean. Additionally, based on ion observations, Pikridas et al. (2012) showed that NPF is more frequent in winter. By using the same data set from eastern Mediterranean, Kalivitis et al. (2012) reported night-time enhancements in ion concentrations with a plausible association with NPF, being among the very few locations where such observations have been made. Manninen et al. (2010) presented an analysis of a full year of observations of NPF with atmospheric ion spectrometers at various locations across Europe during the EUCAARI project and showed that NPF is less frequent in the eastern Mediterranean site than in other, mostly continental, European sites. On the other hand, Berland et al. (2017) showed that similar patterns are being observed throughout the Mediterranean when comparing observations from the island of Crete to a western Mediterranean site in terms of the frequency of occurrence, seasonality, and particle formation and growth rates. Kalivitis et al. (2015) studied for the first time the NPF-CCN link using observations of particle number size distributions, CCN and high-resolution aerosol chemical composition for the eastern Mediterranean atmosphere. From the hygroscopicity of the particles in different size fractions, it was concluded that smaller particles during active NPF periods tend to be less hygroscopic (and richer in organics) than larger ones. Finally, Kalkavouras et al. (2017) reported that NPF may

1 result in higher CCN number concentrations, but the effect on cloud droplet number is limited

2 by the prevailing meteorology.

3 In this work, we present results from the analysis of ten years of aerosol particles number size

4 distributions and more than two years of atmospheric ion size distributions, representing one

5 of the longest published NPF data set in the Mediterranean atmosphere. The main questions

6 we wanted to address were: 1) How often does NPF take place in eastern Mediterranean,

7 what are the characteristics of this phenomenon and to what extent has it changed over the

8 period under study? 2) Are there features in NPF observed at the study area that are not

9 common in other locations? and 3) How well can numerical models, used in different

10 environmental conditions, represent NPF in this subtropical environment?

11 2) Materials and methods

12 2.1) Measurements

13 Measurements presented in this work were carried out at the atmospheric observation

14 station of the University of Crete at Finokalia, Crete, Greece (35˚20′N, 25˚40′E, 250m a.s.l)

15 over ten years, between June 2008 and June 2018. The Finokalia station

16 (http://finokalia.chemistry.uoc.gr/) is a European supersite for aerosol research, part of the

17 ACTRIS (Aerosols, Clouds, and Trace gases Research Infrastructure) Network. The station is

18 located at the top of a hill over the coastline, in the north east part of the island of Crete

19 (Mihalopoulos et al., 1997). The station is representative for the marine background

20 conditions of eastern Mediterranean (Lelieveld et al., 2002), with negligible influence by local

21 anthropogenic sources. The nearest major urban center in the area is Heraklion with

22 approximately 200 000 inhabitants, located about 50 km to the west of the station.

23 In order to monitor the NPF events, a TROPOS type custom-built Scanning Mobility Particle

24 Sizer (SMPS), similar to IFT-SMPS in Wiedensohler et al. (2012), was used at Finokalia. Particle

25 number size distributions were measured in the diameter range of 9−848 nm every five

26 minutes. The system was a closed-loop, with a 5:1 ratio between the aerosol and sheath flow

27 and it consisted of a Kr-85 aerosol neutralizer (TSI 3077), a Hauke medium Differential Mobility

28 Analyzer (DMA) and a TSI-3772 Condensation Particle Counter (CPC). The sampling was made

29 through a PM_{10} sampling head and the sample humidity was regulated below the relative

30 humidity of 40% with the use of Nafion® dryers in both the aerosol and sheath flow. The

31 measured number size distributions were corrected for particle losses by diffusion on the

32 various parts of the SMPS according to the methodology described in Wiedensohler et al.

1 (2012). Three different types of calibration were performed for the SMPS, DMA voltage supply

2 calibration, aerosol and sheath flows calibrations and size calibrations. These measurements

3 have been performed at Finokalia on a continuous basis since 2008. The instrument used at

4 Finokalia was audited on-site with good results in the framework of EUSAAR (European

5 Supersites for Atmospheric Aerosol Research) project (http://www.wmo-gaw-wcc-aerosol-

6 physics.org/audits.html) and has successfully passed twice laboratory intercomparison

7 workshops (2013 and 2016, reports available at http://www.wmo-gaw-wcc-aerosol-

8 physics.org/instrumental-workshops.html) in the framework of ACTRIS project. The

9 instrument has been operated following the recommendations described in Wiedensohler et

10 al. (2012). Additional information for newly formed particles were obtained with the use of

11 an Air Ion Spectrometer (AIS- AIREL Ltd., Institute of Environmental Physics, University of

12 Tartu, Estonia, Mirme et al., 2007). AIS is a cluster ion air spectrometer used to simultaneously

13 measure electrical mobility distribution of positive and negative air ions (mobilities in the

14 range of 2.4 to $1.3 \cdot 10^{-3}$ cm^2 V^{-1} s^{-1}). The mobility distributions were then transformed to size

15 distributions in the size range 0.8-42 nm. The number counting threshold was approximately

16 10 cm^{-3} and the uncertainties of the AIS measurements were ~10% for negative and positive

17 ion concentrations and ~0.5 nm in size (Manninen et al., 2010). The diameter of the AIS inlet

18 tube was 35 mm and the sample flow rate was 60 L m^{-1}. The time step of the measurements

19 was five minutes.

20 These measurements have been used to identify NPF for the whole period and provide a

21 historical perspective for the frequency and the characteristics of NPF phenomena in the

22 eastern Mediterranean. Calculations for formation rates of new particles (J), growth rates (GR)

23 in various size ranges and condensation sink (CS) were made according to Kulmala et al.

24 (2012). Formation rates of particles with diameter D_p (in this study D_p=9 nm) were calculated

25 as:

26 $$J_{Dp} = \frac{\Delta N_{D_p}}{\Delta t} + CoagS \cdot N_{D_p} + \frac{GR}{\Delta D_p} \cdot N_{D_p} + S_{losses} \ (1)$$

27 ΔN_{D_p} is the increase in nucleation mode particles' number concentration (D_p<25 nm), $CoagS$

28 is the coagulation of 9-nm particles on larger particles, GR is the growth rate in the size range

29 9-25 nm. S_{losses} takes into account additional losses and was neglected in this study. GR was

30 calculated using the mode-fitting method (Dal Maso et al., 2005). The aerosol size

31 distributions were fitted with lognormal distributions and the nucleation mode geometric

1   mean diameter was plotted as a function of time. *GR* was calculated as the slope of the linear

2   fit so that:

3 $$GR = \frac{dD_p}{dt} \ (2)$$

4   *CS* is the condensation sink caused by the pre-existing aerosol population and was calculated

5   using the properties of sulfuric acid as condensing vapor.

6   All important meteorological parameters were monitored every five minutes using an

7   automated meteorological station, including the temperature, wind velocity and direction,

8   relative humidity, solar irradiance and precipitation. Ozone concentrations were measured

9   with a TEI 49C instrument and nitrogen oxides with a TEI 42CTL, both commercially available,

10   with a time step of five minutes.

11   2.2) NPF simulations with the MALTE-Box model

12   The simulations of NPF events in the eastern Mediterranean atmosphere were here

13   performed using the MALTE-box model of the University of Helsinki. This 0-d model able to

14   simulate aerosol dynamics and chemical processes has successfully reproduced observations

15   of aerosol formation and growth in the boreal environment (Boy et al., 2006) as well as in

16   highly polluted areas (Huang et al., 2016). For the present study, chemical reactions relevant

17   to the production of condensing species from the Master Chemical Mechanism (MCM) were

18   incorporated in the MALTE-box chemical mechanism, as described in Boy et al. (2013). These

19   include the full MCM degradation scheme of the following volatitle organic compounds

20   (described in more detail in Tzitzikalaki et al., 2017): C_1-C_4 alkanes, C_2-C_3 alkenes, acetylene,

21   isoprene, α- and β-pinene, aromatics, methanol, dimethyl sulfide, formaldehyde, formic and

22   acetic acids, acetaldehyde, glycoaldehyde, glyoxal, methylglyoxal, acetone, hydroxyacetone,

23   butanone and marine amines. The Kinetic PreProcessor (KPP) was used to produce the Fortran

24   code for the calculations of the concentrations of each individual compound (Damian et al.,

25   2002), except for those species whose concentrations were manually input from large scale

26   model simulations.

27   The major aerosol dynamical processes for clear sky atmosphere were simulated by the size-

28   segregated aerosol model UHMA (University Helsinki Multicomponent Aerosol Model,

29   Korhonen et al., 2004) impended in the MALTE-Box model. Measured aerosol number size

30   distributions were used to initialize UHMA daily, which simulates NPF, coagulation, growth

31   and dry deposition of particles. UHMA simulated new cluster formation using the activation

1 nucleation parameterization, so that the nucleation rate has a linear relationship with sulfuric

2 acid concentration, depending on the nucleation coefficient $K_{act.}$

3 Apart from sulfuric acid, about 20 extremely low-volatility organic compounds (ELVOCs) and

4 7 selected semi-volatile organic compounds (SVOCs) were treated as condensing vapors,

5 following the simplified chemical mechanism presented in Huang et al. (2016). All condensing

6 compounds were treated either as sulfuric acid or organic compounds and the condensation

7 of organic vapors was determined by the nano-Kohler theory (Kulmala et al., 2004b).

8 As input to the MALTE-Box model were used the observations at Finokalia station and when

9 such observations were not available, the results from numerical simulations with the global

10 3-dimensional chemistry transport model (CTM) TM4-ECPL (Daskalakis et al., 2015, 2016;

11 Myriokefalitakis et al., 2010, 2016) for Finokalia. Observational data include temperature,

12 relative humidity, total radiation (meteorological input), ozone (O_3) and nitrogen oxides (NOx)

13 concentrations as well as aerosol number size distributions. The aerosol number size

14 distribution measured by the SMPS was used to calculate the condensation sink for H_2SO_4

15 vapors. Due to the lack of detailed measurements of VOC at Finokalia, as a first approximation,

16 biogenic and anthropogenic concentrations of all the above mentioned VOCs resolved every

17 3 hours were taken from the TM4-ECPL model.

18 The global TM4-ECPL model was run driven for this study by ECMWF (European Centre for

19 Medium – Range Weather Forecasts) Interim re–analysis project (ERA – Interim) meteorology

20 (Dee et al., 2011) of the year 2012 at an horizontal resolution of 3° in longitude x 2° in latitude

21 with 34 vertical layers up to 0.1 hPa. The model used year-specific meteorology and emissions

22 of trace gases and aerosols. For this study, that of the year 2012 was used, except for soil NOx

23 and oceanic CO and VOCs emissions which were taken from POET inventory database for the

24 year 2000 (Granier et al., 2005). TM4-ECPL simulations for this work were performed with a

25 model time-step of 30 min, and the simulated VOC concentrations every 3-hours were used

26 as input to MALTE box model; SO_2 surface levels at Finokalia were taken from Monitoring

27 Atmospheric Composition and Climate (MACC) data assimilation system (Inness et al., 2013).

28 For the calculations of the photo-dissociation rate coefficient by the MALTE-Box model, the

29 solar actinic flux (AF) is needed. Unfortunately, AF was not measured at Finokalia in 2012,

30 therefore AF levels were calculated by the Tropospheric Ultraviolet and visible Radiation

31 Model (TUV, Madronich, 1993) version v.5 for cloud free conditions. The ability of TUV to

32 calculate the AF at Finokalia was investigated by comparing observations of photo dissociation

1   rates of O_3 (JO^1D) and NO_2 (JNO_2) and model calculations. The measurements of these photo

2   dissociation rates were performed by filter radiometers (Meteorologie Consult, Germany).

3   The JO^1D was measured at wavelengths <325 nm, while for JNO_2 wavelengths <420 nm were

4   used.

5   A series of sensitivity tests of AF to different input parameters was also performed to optimize

6   the calculations. The model uses extra-terrestrial solar spectral irradiance (200-1000 nm by

7   0.01nm steps) and computes its propagation through the atmosphere taking into account

8   multiple scattering and the absorption and scattering due to gases and particles. TUV inputs

9   of interest were surface reflectivity (albedo), O_3 column, Aerosol Optical Depth at 500 nm

10 (AOD), Single Scattering Albedo of aerosol (SSA), NO_2 column, air density. Total O_3 column

11 values were taken from the Ozone Monitoring Instrument (OMI) on the Aura spacecraft of

12 NASA (Levelt et al., 2006). Aerosol columnar optical properties were obtained from the

13 Aerosol Robotic Network (AERONET). AOD data were measured at the FORTH_Crete station

14 which is located 35 km west of Finokalia (Fotiadi et al., 2006). Data level 1.5 from Version 2

15 were used (cloud-screened). Total NO_2 column values were taken from GOME2 and OMI

16 satellites. The calculations were carried out at wavelength from 280 to 650 nm with a

17 resolution of 5 nm. Simulations using surface reflectivity of 0.075 and simulation using O_3

18 column taken from OMI had the best correlation with measurements. However, the TUV

19 model still significantly overestimated JO^1D and JNO_2 data. Thus, a parameterisation took

20 place following a simple empirical approach, according to Mogensen et al. (2015) and the

21 ratios between the measured and modelled (from TUV) photolysis rate were calculated and

22 used in the model.

23 3) Results and discussion

24 3.1) Particle size distribution and its connection with NPF

25 We analyzed all available measurements of number size distributions of atmospheric aerosol

26 particles measured at Finokalia in order to identify and analyze the NPF phenomenon in the

27 eastern Mediterranean. The data coverage for the period 2008-2018 was 82 %, providing one

28 of the longest time series of size distributions not only in this region but also in the southern

29 Europe and a unique data base for aerosol physical properties.

30 First, we calculated the total particle number concentration (median concentration was

31 2202 cm^{-3}, standard deviation (SD) 528 cm^{-3}) and corresponding number concentration in the

32 nucleation mode (D_p<25 nm, median 80 cm^{-3}, SD 528 cm^{-3}), Aitken mode (25 nm<D_p<100 nm,

median 1028 cm^{-3}, SD 894 cm^{-3}) and accumulation mode (D_p>100 nm, median 898 cm^{-3}, SD 605 cm^{-3}). We found that Aitken mode accounted for 50% and accumulation mode 42% of the total particle number concentration, while the nucleation mode accounted only for 8%. The standard deviation of the nucleation particle number concentration was 528 cm^{-3}, indicating that the abundance of these smallest particles is of episodic nature. The highest monthly average concentrations of nucleation mode particles were observed during winter and early spring and the lowest ones during summer (Fig. 1a). Calculating the median diurnal variability of the nucleation mode, we can see that there is a clear pattern for all seasons of the year (Fig. 2a) with a sudden burst in the number concentration around noon that is most pronounced in winter and least in summer. Such an observation suggests that the nucleation particle number concentration is controlled by NPF episodes rather than other sources such as combustion processes. As can be seen in Fig. 2b where a typical "banana shaped" pattern of an NPF event at Finokalia is presented, the sudden burst at noon is typical for a NPF event. In summer, nucleation mode particles have the highest concentrations during the night, yet another concentration relative maximum at noon can be attributed to NPF (Fig. 2a). The shift in the average time of the daytime burst of nucleation mode particles can be attributed to the annual variation of the daylight length. Similar observations to ours have been reported in Cusack et al. (2013) for the western Mediterranean where the diurnal variation of nucleation mode particles presents a clear maximum at noon under both polluted and clean conditions.

It is worth noticing that during night-time the median nucleation mode particle number concentrations were similar in all the seasons. This suggests that there is some new particle production mechanism at night, especially in summer and autumn, that operates separately from daytime NPF. Frequently during the night-time, we observed a pronounced appearance of new nucleation mode particles over several hours as illustrated by Fig. 3. While nocturnal NPF has been reported in the literature (see Salimi et al. (2017) and references therein), this phenomenon seems to be rare and it remains unclear what are the exact mechanisms leading to it. Given that we observed no or little growth during nighttime NPF, we may   assume that the sources leading to the formation of new particles are local rather than regional and that the lack of photochemistry during night limits the abundance of condensable vapors driving particle growth. Observations of very localized NPF have been reported in Mace Head, Ireland, where intense NPF frequently takes place under low tide conditions when algae are exposed to the atmosphere (O'Dowd et al., 2002). Henceforth, we will exclude the nighttime NPF events from our further analysis. We refer the interested reader to Kalivitis et al. (2012) for a more detailed description of this phenomenon.

Overall, we observed atmospheric NPF to take place during both day and night at Finokalia, but no sign of any other source of nucleation mode particles in measured air masses. We therefore hypothesize that atmospheric NPF is the dominant source of nucleation mode particles in this Mediterranean environment.

3.2) Characteristics of NPF in the eastern Mediterranean

We analyzed the dataset of aerosol size distributions following the approach of Dal Maso et al. (2005) in order to mark the available days as 1) NPF event days when a clear new nucleation mode and subsequent growth of newly-formed particles to larger diameters can be observed, 2) non-event days and 3) undefined days when either new particles appear into the Aitken mode or nucleation mode particles do not show a clear growth. The available days were manually inspected and classified.

We used the Statistica software package for Windows to carry out factor analyses, including meteorological parameters, ozone concentrations (as an important oxidant in the atmosphere) and PM_{10} mass concentration (as an index of particulate pollutant levels), in order to examine whether any of these factors were associated with the formation of new particles, represented by the nucleation mode number concentration. Furthermore, we divided our data to night and day time periods in order to separate daytime NPF from that taking place during nighttime. The only parameter that had some effect on the nucleation mode particle number concentration was the wind velocity: when strong winds were prevailing at Finokalia, it was more unlikely to observe nucleation particles. On the other hand, the lack of correlation to any other parameter may indicate that the NPF is not sensitive to local meteorological conditions, preexisting particulate matter and ozone levels in this environment. Air mass back trajectories calculated using the HYSPLIT model showed little difference during NPF events from air masses typical for the prevailing situation at Finokalia: air masses arriving at Finokalia from the northeast were the most frequent during NPF events (30% against 24% of all days), followed by northern directions (20% against 21%) and northwestern air masses that were more frequent than the average (19% against 17%).

Next, we focused on determining the main characteristics of daytime NPF at Finokalia. Overall, 837 NPF events were identified. This is one of the longest time series of the NPF phenomenon recorded in the Mediterranean atmosphere, providing a representative climatology of NPF events in this region. NPF took place 27% of the 3057 available measurement days whereas no event occurred on 50% of those days. It is worth noting that 23% of the days were

characterized as undefined, which means that while no clear NPF event could be observed, there was some evidence of secondary particle formation although not at the immediate vicinity of the station (Table 1). We found that NPF is most frequent in April and May, probably due to the biogenic activity and the onset of intense photochemistry, and least frequent in August (Fig. 4) probably due to high wind speeds occurring these month (not shown) and additionally the high Condensational Sink (Fig. 1b). Rain season in southeastern Europe in early autumn leads to gradual CS decrease, and as a result a local maximum in NPF frequency is observed in October. NPF at Finokalia takes place throughout the year.

As a next step, we classified the NPF events into Class I or Class II events depending on whether the particle formation rate at 9 nm (J_9) and growth rates from 9 to 25 nm diameter (GR_{9-25}) could be calculated with a good confidence or not respectively. Overall, Class I events corresponded to 8% of the available measuring days and 28% of the event days, and they were observed throughout the year, providing enough data for a statistical analysis of particle formation and growth rates during NPF events (Fig. 5).

The average value of J_9 during the Class I NPF events in Finokalia was 0.9 cm^{-3} s^{-1} (median 0.5 cm^{-3} s^{-1}, SD 1.2 cm^{-3} s^{-1}). This is well in the range of values reported for J_{10} in other locations (Kulmala et al., 2004a), higher though than J_{16} reported by Berland et al. (2017) at the Finokalia site in 2013 (0.26 cm^{-3} s^{-1}), but substantially lower than the values found by Kopanakis et al. (2013) in western Crete (13.1 ± 9.9 cm^{-3} s^{-1}). The monthly variation of J_9 (Fig. 6a) shows that the highest average formation rates were observed in December and January, probably as a result of the low CS values observed in winter, although it is difficult to say which factors determine the monthly variability of J_9 at Finokalia. Seasonal averages of J_9, GR_{9-25} and CS are summarized in Table 2. Moreover, we found that J_9 and N_{9-25} have a clear linear relation (Fig. 7), which supports our earlier hypothesis that at Finokalia the main source of nucleation mode particles is their secondary formation in the atmosphere.

We calculated the average growth rate of the newly formed particles to be 5.4 nm hr^{-1} (median 4.5 nm hr^{-1}, SD 3.9 nm hr^{-1}). We found that GR_{9-25} is highest in summer until September and lowest in winter and early spring, probably in line with the seasonal cycle of photochemical activity and biogenic emission patterns, producing condensable species that are driving the growth process (Fig. 6b). Additionally, transported pollution in summer at Finokalia may contribute except of CS to GR as well, since transported anthropogenic SO_2 is a precursor for condensable sulfuric acid.

The survival probability of newly-formed particles is closely related to the ratio of CS to GR, at least for cluster sizes (Kerminen and Kulmala, 2002; Kulmala et al., 2017) and at Finokalia they present the same annual cycle. The survival probability for nucleation mode particles for Class I events was calculated based on the formula in Kulmala et al. (2017). It was found that on a seasonal basis the median survival probability is higher in summer and winter, however varies between the seasons only within 5%. The concentrations of nucleation mode particles are lower during summer and the average duration of the NPF in summer seems to be shorter as shown in Fig. 1 and 2a respectively. These observations may be explained by the higher CS and GR during summer. The CS (and hence $CoagS$) may directly affect the maximum concentrations observed. The slightly higher survival probability in summer perhaps explains that given high CS values, new particles need to grow fast in order to survive. On the other hand, one would expect NPF to be most frequent in winter when the highest concentrations of nucleation particles are observed and CS is the lowest, however this was not the case. A possible explanation for the high nucleation mode particle number concentrations in winter could be that the survival probability is higher than in spring or autumn.

3.3) NPF trends during the 2008-2018 period

During the period under study no statistically significant trends in NPF events were observed at Finokalia for the 120 available months. It should be noted though, that since 2010 a decreasing trend is observed, which is statistically significant with a p-value of 0.005. During the measurement period under study, no trend in J_9 was observed (Fig. 8c). Although no statistically significant trend was observed for GR_{9-25} as well (Fig. 8d), we observed a decreasing trend during the period 2008-2015 of about 0.3 nm hr^{-1} yr^{-1}. This trend can be considered statistically significant (p-value of 0.03). In order to explain this trend, we need to emphasize the regional characteristics of the observations at Finokalia, as this site is greatly affected by long-range transported pollutants of marine, desert dust and polluted continental origin (Lelieveld et al., 2002). Non-sea salt sulfate (nss-SO_4^{2-}) can be considered as an indicator of regional pollution from anthropogenic activities (SO_2 emissions), and since the beginning of the economic crisis in Europe, especially in Greece, we observed a clear decline in its concentration since 2008 (Paraskevopoulou et al., 2015) which however has stopped after 2015. We can therefore assume also a regional decrease in SO_2 emissions, since the main source of SO_2 at Finokalia is attributed to transported pollution (Sciare et al., 2003). This could

result in a decrease in the availability of sulfuric acid, a major condensable species responsible for the particle growth (Bzdek et al., 2012).

Hamed et al. (2010) studied the effect of the reduction in anthropogenic SO_2 emissions in Germany between the years 1996-97 and 2003-06 as a result of the socio-economic changes in East Germany after the reunification. They observed a notable decrease in the NPF event frequency but an increase in the growth rate of nucleated particles. A decrease in the NPF frequency due to the reduction of anthropogenic SO_2 emissions in eastern Lapland was also reported by Kyrö et al. (2014), and this decrease was most pronounced for the Class I NPF events. Nieminen et al. (2014) analyzed the longest data set reported in literature from Finland and found that, despite major decreases in ambient SO_2 concentrations observed all over Europe as a result of overall air quality improvements, there was a slight upward trend in the particle formation and growth rates. This feature was attributed partly to increased biogenic emissions over the same period.

In our case the reasons for the variations in the NPF frequency, J_9 and GR_{9-25} remain unclear, even though factors like meteorological conditions and organic vapor abundance have probably played some role in this respect.

3.4) Atmospheric ion observations related to new particle formation

At the Finokalia station, atmospheric ion observations relevant to new particle formation were performed during two separate periods, 2008-2009 during the EUCAARI project (Manninen et al., 2010) and 2012-2014 during the FRONT (Formation and growth of atmospheric nanoparticles) project. Here we will focus only on FRONT data, since the EUCAARI dataset is discussed in detail in Manninen et al. (2010) and Pikridas et al., (2012). A typical nucleation event is presented in Fig. 9 as recorded by both the AIS and SMPS. AIS observations may provide information about the initial stages of new particle formation as particles can be observed emerging in the intermediate ion diameter range 1.6-7.4 nm. Intermediate ions appear only under certain circumstances, such as during precipitation, at high wind speeds, and when NPF is taking place (Hõrrak et al. 1998; Tammet et al., 2014; Leino et al., 2016; Chen et al., 2017). In the following we will focus on NPF and use only the observations from the negative polarity due to the better representation of NPF events in those data compared with corresponding positive ions in our dataset (Kalivitis et al., 2012).

We classified all of the available AIS measurement days into event, non-event and undefined days, once again according to methods introduced by Dal Maso et al. (2005), and subsequently

compared the findings from AIS data to those from the SMPS. In Fig. 9 an NPF event is presented observed with both the AIS and the SMPS at Finokalia. Surprisingly, the two data sets for the same time period gave quite different results in terms of the NPF event frequency: in the AIS data the NPF event frequency peaked earlier during the year than in the SMPS data (Fig. 10). This feature was evident in both periods of AIS measurements and has been also reported at a rural site in Hungary (Yli-Juuti et al., 2009), probably because AIS detects only naturally charged particles while SMPS detects all particles. Additionally, it is possible that AIS data are more representative of local NPF events with limited particle growth, and such events may not be seen in the SMPS data. On the other hand, the SMPS measures neutral particles but has a much higher detection limit (9 nm), so its data may be more representative of regional NPF that takes place over distances of hundreds of kilometers (Kalkavouras et al., 2017).

We calculated the growth rates at three different size ranges for the FRONT project similarly to Manninen et al. (2010) and Pikridas et al (2012) for the EUCAARI project data. The particle growth rates in the size ranges 1.5-3 nm, 3-7 nm and 7-20 nm were 1.6 ±1.8 nm hr^{-1}, 5.4±4.9 nm hr^{-1} and 9.1±9.5 nm hr^{-1}, respectively. These values are lower than those in Pikridas et al. (2012) but comparable to those observed during the EUCAARI project for the first two size ranges, and higher than those observed during the EUCAARI project for the last size range (Manninen et al., 2010). Overall, we observed much faster growth of newly-formed charged particles in the eastern Mediterranean atmosphere after their first growth steps beyond 3 nm in diameter, reflecting probably the strong Kelvin effect at small particle sizes preventing condensation and hence growth, and the abundance of precursors leading to nucleation and condensing species contributing to each growth stage.

3.5) Simulations of NPF using the zero-dimensional model MALTE-box

In order to evaluate our understanding of the observed NPF events in the eastern Mediterranean we chose to simulate two distinct cases of one week duration each, during which NPF events have been observed (event week) or not (no event week). The selection was done from the summer of the year 2012, when JO^1D and JNO_2 photodissociation measurements were also available at Finokalia. Two weeks in August 2012 were chosen, 28/08– 03/09 as event week and 09/08– 15/08 as non-event week. The "event week" was described in detail by Kalivitis et al. (2015). Applying the MALTE-Box model the aerosol size distribution and its evolution over the week has been simulated for these two cases.

During the ''event week'' the simulated formation of new particles successfully coincided with the observations. The NPF events simulated using the nucleation rates as parameterized for the boreal environment overestimated the observations while the simulated growth of newly-formed particles was greatly underestimated as shown in Tzitzikalaki et al. (2017). The most likely reason for this is the very low concentration of monoterpenes, calculated by TM4-ECPL global model for the Finokalia model grid box, on which the ELVOC and SVOC chemistry was built on. Indeed, the TM4-ECPL model results for Finokalia were too low compared to monoterpenes observations in 2014 (not shown). Therefore, we performed a number of sensitivity tests to improve the simulations by adjusting the nucleation coefficient and the monoterpene concentrations until we simulated efficiently the nucleation and growth rates observed during the second day of the "event week" when the most pronounced NPF event was observed. The best agreement between model results and observations was reached by decreasing the nucleation coefficient from $10^{-11}\,s^{-1}$ (the value commonly used for the boreal environment) to $5\times10^{-16}\,s^{-1}$ and increasing by a factor of 10 the α- and β-pinene concentrations. With these modifications the model results improved and the aerosol number size distributions were better simulated, as well as total number and volume concentration of aerosol particles (Fig. 11a and b respectively). This was the first time that we were able to simulate NPF in the eastern Mediterranean environment. The almost five orders of magnitude lower nucleation coefficient used here for the sub-tropical set-up could be related to the contribution of still unknown compounds in the cluster-formation process. Huang et al. (2016) applied different kinetic nucleation coefficients at Nanjing, China, with the lowest value for a "China-clean" day of $6.0 \times 10^{-13}\,s^{-1}$. The higher monoterpene concentrations used are comparable to the findings at Finokalia but also at another location in the eastern Mediterranean (Debevec et al., 2018).

Using the non-event week as our control case, we performed simulations of number size distributions at Finokalia station using the sub-tropical set-up and compared it to our measurements. For the "non-event week", weak NPF were predicted by the model during the last two days that were not found in the measurements (Tzitzikalaki et al., 2017) but appear to be associated with the rapid drop of *CS* during day five of the simulations. Nevertheless, even if no NPF took place during the last two days, it was apparent in our measurements that some nucleation particles appeared (~200 cm^{-3}) and thus the general tendency was captured by the model. Both total number and volume concentrations were adequately simulated by the model (Fig. 12 a, b). These results show the potential of MALTE-box model to simulate the NPF in the eastern Mediterranean and the importance of input data. Therefore, when more

appropriate input data for Malte-box will become available (concurrent detailed measurements of gases and aerosol distributions) at Finokalia, new simulations and VOC measurements will further provide insight in the nucleation mechanisms, the growth process and the factors controlling NPF in the eastern Mediterranean atmosphere.

4) Conclusions

NPF in the atmosphere is a recurrent phenomenon in eastern Mediterranean. In this study, we presented the longest time series of NPF records in the region. We analyzed 3057 days of aerosol number size distribution data from June 2008 until June 2018 and found that NPF took place 27% of the available days, more frequently in spring and less frequently in late summer. Production of nucleation mode particles was common during night-time as well. Nucleation mode particle number concentrations were low outside periods of active NPF and subsequent particle growth indicating absence of local sources. Classification of NPF events based on atmospheric ion measurements differed from the corresponding classification based on mobility spectrometer measurements: the maximum frequency of NPF events was observed earlier in spring from AIS data than from SMPS data, possibly indicating a different representation of local and regional NPF events between these two data sets since SMPS measures new particles after they have grown to diameters larger than 9-nm and hence records only regional events lasting for several hours.

We used the MALTE-box model to simulate NPF observations in the eastern Mediterranean region. Using a "sub-tropical" environment parametrization, we were able to simulate with good agreement the selected time period. The parametrization used was significantly different than the one used for the boreal environment: nucleation rates were much lower, yet monoterpenes seemed to play a key role in the mechanisms governing NPF phenomena.

From the results presented in this work it is evident that the Finokalia site is a unique location in the eastern Mediterranean for studying the processes leading to NPF in the marine environment. As a next step, a more detailed look to the precursors driving these processes is necessary, with special emphasis on VOCs, and the expansion of the available measurements at the site in order to eliminate the uncertainties introduced in our simulations from the use of model outputs instead of observations.

5) Author contribution

N.K., G.K., I.S., A.B., P.K. and H.E.M. participated in the field measurements and analyzed the data, E.T., N.D., S.M., P.R. and M.B. participated in the modeling study, T.P.,V.M.K., M.K., M.K. and N.M. contributed to the manuscript preparation.

6) Acknowledgements

The research project was implemented within the framework of the Action «Supporting Postdoctoral Researchers» of the Operational Program "Education and Lifelong Learning" (Action's Beneficiary: General Secretariat for Research and Technology), and was co-financed by the European Social Fund (ESF) and the Greek State. This research is supported by the Academy of Finland Center of Excellence program (project number 1118615). We acknowledge funding from the EU FP7-ENV-2013 program "impact of Biogenic vs. Anthropogenic emissions on Clouds and Climate: towards a Holistic UnderStanding" (BACCHUS), project no. 603445 and the Horizon 2020 research and innovation programme ACTRIS-2 Integrating Activities (grant agreement No. 654109). This study contributes to ChArMEx work package 1 on aerosol sources. We acknowledge support of this work by the project "PANhellenic infrastructure for Atmospheric Composition and climatE change" (MIS 5021516) which is implemented under the Action "Reinforcement of the Research and Innovation Infrastructure", funded by the Operational Programme "Competitiveness, Entrepreneurship and Innovation" (NSRF 2014-2020) and co-financed by Greece and the European Union (European Regional Development Fund).

1 7) References

2 Berland, K., Rose, C., Pey, J., Culot, A., Freney, E., Kalivitis, N., Kouvarakis, G., Cerro, J. C.,

3 Mallet, M., Sartelet, K., Beckmann, M., Bourriane, T., Roberts, G., Marchand, N.,

4 Mihalopoulos, N., and Sellegri, K.: Spatial extent of new particle formation events over the

5 Mediterranean Basin from multiple ground-based and airborne measurements, Atmos. Chem.

6 Phys., 17, 9567-9583, https://doi.org/10.5194/acp-17-9567-2017, 2017.

7 Boy, M., Hellmuth, O., Korhonen, H., Nillson, D., ReVelle, D., Turnipseed, A., Arnold, F. and

8 Kulmala, M.: MALTE – Model to predict new aerosol formation in the lower troposphere,

9 Atmos. Chem. Phys., 6, 4499–4517, doi:10.5194/acp-6-4499-2006, 2006.

10 Boy, M., Mogensen, D., Smolander, S., Zhou, L., Nieminen, T., Paasonen, P., Plass-Dülmer, C.,

11 Sipilä, M., Petäjä, T., Mauldin, L., Berresheim, H., and Kulmala, M.: Oxidation of SO_2 by

12 stabilized Criegee intermediate (sCI) radicals as a crucial source for atmospheric sulfuric acid

13 concentrations, Atmos. Chem. Phys., 13, 3865-3879, https://doi.org/10.5194/acp-13-3865-

14 2013, 2013.

15 Bzdek, B. R., Zordan, C. A., Pennington, M. R., Luther, G. W., and Johnston, M. V.: Quantitative

16 Assessment of the Sulfuric Acid Contribution to New Particle Growth. Environmental Science

17 & Technology, 46, 4365–4373. http://doi.org/10.1021/es204556c, 2012.

18 Chen, X., Virkkula, A., Kerminen, V.-M., Manninen, H. E., Busetto, M., Lanconelli, C., Lupi, A.,

19 Vitale, V., Del Guasta, M., Grigioni, P., Väänänen, R., Duplissy, E.-M., Petäjä, T., and Kulmala,

20 M.: Features of air ions measured by an air ion spectrometer (AIS) at Dome C, Atmos. Chem.

21 Phys., 17, 13783-13800, 2017.

22 Cusack, M., Pérez, N., Pey, J., Wiedensohler, A., Alastuey, A., and Querol, X.: Variability of sub-

23 micrometer particle number size distributions and concentrations in the Western

24 Mediterranean regional background. Tellus B, 65.

25 doi:http://dx.doi.org/10.3402/tellusb.v65i0.19243, 2013.

26 Dall'Osto, M., Beddows, D. C. S., Asmi, A., Poulain, L., Hao, L., Freney, E., Allan, J D.,

27 Canagaratna, M., Crippa, M., Bianchi, F., de Leeuw, G., Eriksson, A., Swietlicki, E., Hansson, H

28 C., Henzing, J S., Granier, C., Zemankova, K., Laj, P., Onasch, T., Prevot, A., Putaud, J P., Sellegri,

29 K., Vidal, M., Virtanen, A., Simo, R, Worsnop, D., O'Dowd, C.,Kulmala, M. and Harrison, R.

M.:Novel insights on new particle formation derived from a pan-european observing system. Scientific Reports, 8(1), 1482. http://doi.org/10.1038/s41598-017-17343-9, 2018.

Dal Maso, M., Kulmala, M., Riipinen, I., Wagner, R., Hussein, T., Aalto, P. P., and Lehtinen, K. E. J.: Formation and growth of fresh atmospheric aerosols: eight years of aerosol size distribution data from SMEAR II, Hyytiälä, Finland, Boreal Environ. Res., 10, 323–336, 2005.

Damian, V., Sandu, A., Damian, M., Potra, F., and Carmichael, G. R.: The kinetic preprocessor KPP-a software environment for solving chemical kinetics, Computers & Chemical Engineering, 26, 1567–1579, http://doi.org/10.1016/S0098-1354(02)00128-X, 2002.

Daskalakis, N., Myriokefalitakis, S., and Kanakidou, M.: Sensitivity of tropospheric loads and lifetimes of short lived pollutants to fire emissions, Atmos. Chem. Phys., 15, 3543-3563, https://doi.org/10.5194/acp-15-3543-2015, 2015.

Daskalakis, N., Tsigaridis, K., Myriokefalitakis, S., Fanourgakis, G. S., and Kanakidou, M.: Large gain in air quality compared to an alternative anthropogenic emissions scenario, Atmos. Chem. Phys., 16, 9771-9784, doi:10.5194/acp-16-9771-2016, 2016.

Debevec, C., Sauvage, S., Gros, V., Sellegri, K., Sciare, J., Pikridas, M., Stavroulas, I., Leonardis, T., Gaudion, V., Depelchin, L., Fronval, I., Sarda-Esteve, R., Baisnée, D., Bonsang, B., Savvides, C., Vrekoussis, M., and Locoge, N.: Driving parameters of biogenic volatile organic compounds and consequences on new particle formation observed at an eastern Mediterranean background site, Atmos. Chem. Phys., 18, 14297-14325, https://doi.org/10.5194/acp-18-14297-2018, 2018.

Dee, D. P., Uppala, S. M., Simmons, A. J., Berrisford, P., Poli, P., Kobayashi, S., and Vitart, F.: The ERA-Interim reanalysis: configuration and performance of the data assimilation system, Quarterly Journal of the Royal Meteorological Society, 137, 553–597. http://doi.org/10.1002/qj.828, 2011.

Fotiadi, A., Hatzianastassiou, N., Drakakis, E., Matsoukas, C., Pavlakis, K. G., Hatzidimitriou, D., Gerasopoulos, E., Mihalopoulos, N., and Vardavas, I.: Aerosol physical and optical properties in the eastern Mediterranean Basin, Crete, from Aerosol Robotic Network data, Atmos. Chem. Phys., 6, 5399-5413, https://doi.org/10.5194/acp-6-5399-2006, 2006.

Gordon, H., Kirkby, J., Baltensperger, U., Bianchi, F., Breitenlecher, M., Curtius, J., Dias, A., Dommen, J., Donahue, N. M., Dunne, E. M., Duplissy, J., Ehrhart, S., Flagan, R. C., Frege, C.,

Fuchs, C., Hansel, A., Hoyle, C. R., Kulmala, M., Kürten, A., Lehtipalo, K., Makhmutov, V., Molteni, U., Rissanen, M. P., Stozhkov, Y., Tröstl, J., Tsagkogeorgas, G., Wagner, R., Williamson, C., Wimmer, D., Winkler, P. M., Yan, C., and Carslaw, K. S.: Causes and importance of new particle formation in the present-day and preindustrial atmospheres, J. Geophys. Res. Atmos., 122, 8739-8760, 2017.

Granier, C., Guenther, A., Lamarque, J., Mieville, A., Müller, J., Olivier, J., Orlando, J., Peters, J., Petron, G., Tyndall, G., and Wallens, S.: POET, a database of surface emissions of ozone precursors, available at: http://www.aero.jussieu.fr/projet/ ACCENT/POET.php, 2005.

Hamed, A., Birmili, W., Joutsensaari, J., Mikkonen, S., Asmi, A., Wehner, B., Spindler, G., Jaatinen, A., Wiedensohler, A., Korhonen, H., Lehtinen, K. E. J., and Laaksonen, A.: Changes in the production rate of secondary aerosol particles in Central Europe in view of decreasing SO_2 emissions between 1996 and 2006, Atmos. Chem. Phys., 10, 1071-1091, https://doi.org/10.5194/acp-10-1071-2010, 2010.

Hõrrak U., Salm J., and Tammet H.: Bursts of intermediate ions in atmospheric air, J. Geophys. Res., 103, 13909–13915, doi: 10.1029/97JD01570, 1998.

Huang, X., Zhou, L., Ding, A., Qi, X., Nie, W., Wang, M., Chi, X., Petäjä, T., Kerminen, V.-M., Roldin, P., Rusanen, A., Kulmala, M., and Boy, M.: Comprehensive modelling study on observed new particle formation at the SORPES station in Nanjing, China, Atmos. Chem. Phys., 16, 2477-2492, https://doi.org/10.5194/acp-16-2477-2016, 2016.

Inness, A., Baier, F., Benedetti, A., Bouarar, I., Chabrillat, S., Clark, H., Clerbaux, C., Coheur, P., Engelen, R. J., Errera, Q., Flemming, J., George, M., Granier, C., Hadji-Lazaro, J., Huijnen, V., Hurtmans, D., Jones, L., Kaiser, J. W., Kapsomenakis, J., Lefever, K., Leitão, J., Razinger, M., Richter, A., Schultz, M. G., Simmons, A. J., Suttie, M., Stein, O., Thépaut, J.-N., Thouret, V., Vrekoussis, M., Zerefos, C., and the MACC team: The MACC reanalysis: an 8 yr data set of atmospheric composition, Atmos. Chem. Phys., 13, 4073-4109, https://doi.org/10.5194/acp-13-4073-2013, 2013.

Kalivitis, N., Birmili, W., Stock, M., Wehner, B., Massling, A., Wiedensohler, A., Gerasopoulos, E., and Mihalopoulos, N.: Particle size distributions in the eastern Mediterranean troposphere, Atmos. Chem. Phys., 8, 6729-6738, doi:10.5194/acp-8-6729-2008, 2008.

Kalivitis N., Stavroulas I., Bougiatioti A., Kouvarakis G., Gagné S., Manninen H.E., Kulmala M., and Mihalopoulos N.: Night-time enhanced atmospheric ion concentrations in the marine boundary layer, Atmos. Chem. Phys., 12, 3627-3638, doi:10.5194/acp-12-3627-2012, 2012.

Kalivitis, N., Kerminen, V.-M., Kouvarakis, G., Stavroulas, I., Bougiatioti, A., Nenes, A., Manninen, H. E., Petäjä, T., Kulmala, M., and Mihalopoulos, N.: Atmospheric new particle formation as a source of CCN in the eastern Mediterranean marine boundary layer, Atmos. Chem. Phys., 15, 9203-9215, doi:10.5194/acp-15-9203-2015, 2015.

Kalkavouras, P., Bossioli, E., Bezantakos, S., Bougiatioti, A., Kalivitis, N., Stavroulas, I., Kouvarakis, G., Protonotariou, A. P., Dandou, A., Biskos, G., Mihalopoulos, N., Nenes, A., and Tombrou, M.: New particle formation in the southern Aegean Sea during the Etesians: importance for CCN production and cloud droplet number, Atmos. Chem. Phys., 17, 175-192, https://doi.org/10.5194/acp-17-175-2017, 2017.

Kerminen, V.-M. and Kulmala, M.: Analytical formulae connecting the "real" and the "apparent" nucleation rate and the nuclei number concentration for atmospheric nucleation events, J. Aerosol Sci., 33, 609-622, 2002.

Kerminen, V.-M., Paramonov, M., Anttila, T., Riipinen, I., Fountoukis, C., Korhonen, H., Asmi, E., Laakso, L., Lihavainen, H., Swietlicki, E., Svenningsson, B., Asmi, A., Pandis, S. N., Kulmala, M., and Petäjä, T.: Cloud condensation nuclei production associated with atmospheric nucleation: a synthesis based on existing literature and new results, Atmos. Chem. Phys., 12, 12037– 12059, doi:10.5194/acp-12-12037-2012, 2012.

Kopanakis, I., Chatoutsidou, S. E., Torseth, K., Glytsos, T., and Lazaridis, M.: Particle number size distribution in the eastern Mediterranean: Formation and growth rates of ultrafine airborne atmospheric particles, Atmospheric Environment, 77, 790–802. http://doi.org/10.1016/j.atmosenv.2013.05.066, 2013.

Korhonen, H., Lehtinen, K. E. J., and Kulmala, M.: Multicomponent aerosol dynamics model UHMA: model development and validation, Atmos. Chem. Phys., 4, 757-771, https://doi.org/10.5194/acp-4-757-2004, 2004.

Kulmala, M., Vehkaṁaki, H., Peẗaja, T., Dal Maso, M., Lauri, A., Kerminen, V.-M., Birmili, W., and McMurry, P. H.: Formation and growth rates of ultrafine atmospheric particles: A review of observations, J. Aerosol Sci., 35, 143–176, 2004a.

1 Kulmala, M, Kerminen, V.-M., Anttila, T., Laaksonen, A. and O'Dowd, C. D: Organic aerosol
2 formation via sulphate cluster activation, J. Geophys. Res., 109, 4205,
3 doi:10.1029/2003JD003961, 2004b.

4 Kulmala, M., Petäjä, T., Nieminen, T., Sipilä, M., Manninen, H. E., Lehtipalo, K., Kerminen, V.-
5 M.: Measurement of the nucleation of atmospheric aerosol particles, Nature Protocols, 7,
6 1651, http://dx.doi.org/10.1038/nprot.2012.091, 2012.

7 Kulmala, M., Petäjä, T., Ehn, M., Thornton, J., Sipilä, M., Worsnop, D. R., and Kerminen, V.-M.:
8 Chemistry of atmospheric nucleation: On the recent advances on precursor characterization
9 and atmospheric cluster composition in connection with atmospheric new particle formation,
10 Annu. Rev. Phys. Chem., 65, 21-37, 2014.

11 Kulmala, M., Kerminen, V.-M., Petäjä, T., Ding, A. J., and Wang L.: Atmospheric gas-to-particle
12 conversion: why NPF events are observed in megacities?, Faraday Discuss., 200, 271-288,
13 doi:10.1039/c6fd00257a, 2017.

14 Kyrö, E.-M., Väänänen, R., Kerminen, V.-M., Virkkula, A., Petäjä, T., Asmi, A., Dal Maso, M.,
15 Nieminen, T., Juhola, S., Shcherbinin, A., Riipinen, I., Lehtipalo, K., Keronen, P., Aalto, P. P.,
16 Hari, P., and Kulmala, M.: Trends in new particle formation in eastern Lapland, Finland: effect
17 of decreasing sulfur emissions from Kola Peninsula, Atmos. Chem. Phys., 14, 4383-4396,
18 https://doi.org/10.5194/acp-14-4383-2014, 2014.

19 Lazaridis, M., K. Eleftheriadis, J. Smolik, I. Colbeck, G. Kallos, Y. Drossinos, V. Zdimal, Z. Vecera,
20 N. Mihalopoulos, P. Mikuska, C. Bryant, C. Housiadas, A. Spyridaki, M. Astitha and V. Havranek:
21 Dynamics of fine particles and photo-oxidants in the eastern Mediterranean (SUB-AERO),
22 Atmospheric Environment, 40, P 6214-6228,
23 http://dx.doi.org/10.1016/j.atmosenv.2005.06.050, 2006.

24 Lehtipalo, K., Rondo, L., Kontkanen, J., Schobesberger, S., Jokinen, T., Sarnela, N., Kürten, A.,
25 Ehrhart, S., Franchin, A., Nieminen, T., Riccobono, F., Sipilä, M., Yli-Juuti, T., Duplissy, J.,
26 Adamov, A., Ahlm, L., Almeida, J., Amorim, A., Bianchi, F., Breitenlechner, M., Dommen, J.,
27 Downard, A. J., Dunne, E. M., Flagan, R. C., Guida, R., Hakala, J., Hansel, A., Jud, W.,
28 Kangasluoma, J., Kerminen, V.-M., Keskinen, H., Kim, J., Kirkby, J., Kupc, A., Kupiainen-Määttä,
29 O., Laaksonen, A., Lawler, M. J., Leiminger, M., Mathot, S., Olenius, T., Ortega, I. K., Onnela,
30 A., Petäjä, T., Praplan, A., Rissanen, M. P., Ruuskanen, T., Santos, F. D., Schallhart, S.,
31 Schnitzhofer, R., Simon, M., Smith, J. N., Tröstl, J., Tsagkogeorgas, G., Tomé, A., Vaattovaara,

P., Vehkamäki, H., Vrtala, A. E., Wagner, P. E., Williamson, C., Wimmer, D., Winkler, P. M., Virtanen, A., Donahue, N. M., Carslaw, K. S., Baltensperger, U., Riipinen, I., Curtius, J., Worsnop, D. R., and Kulmala, M.: The effect of acid-base clustering and ions on the growth of atmospheric nano-particles, Nat. Commun., 7, 11594, doi:10.1038/ncomms11594, 2016.

Leino, K., Nieminen, T., Manninen, H.E., Petäjä, T., Kerminen, V.-M., and Kulmala, M.: Intermediate ions as a strong indicator for new particle formation bursts in a boreal forest. Boreal Env. Res. 21: 274–286, 2016.

Lelieveld, J., Berresheim, H., Borrmann, S., Crutzen, P., Dentener, F., Fischer, H., Feichter, J., Flatau, P., Heland, J., Holzinger, R., Korrmann, R., Lawrence, M., Levin, Z., Markowicz, K., Mihalopoulos, N., Minikin, A., Ramanathan, V., de Reus, M., Roelofs, G., Scheeren, H., Sciare, J., Schlager, H., Schultz, M., Siegmund, P., Steil, B., Stephanou, E., Stier, P., Traub, M., Warneke, C., Williams, J., and Ziereis, H.: Global air pollution crossroads over the Mediterranean, Science, 298, 794–799, doi: 10.1126/science.1075457, 2002.

Levelt, P. F., van den Oord, G. H. J., Dobber, M. R., Malkki, A., Visser, H., de Vries, J., Stammes, P., Lundell, J. O. V., and Saari, H.: The Ozone Monitoring Instrument, IEEE T. Geosci. Remote, 44, 1093–1101, doi: 10.1109/TGRS.2006.872333, 2006.

Madronich, S.: The atmosphere and UV-B radiation at ground level. Environmental UV Photobiology, Plenum Press, 1–39, 1993.

Manninen, H.E., Nieminen, T., Asmi, E., Gagné, S., Häkkinen, S., Lehtipalo, K., Aalto, P., Kivekäs ,N., Vana, M., Mirme, A., Mirme, S., Hõrrak, U., Plass-Dülmer, C., Stange, G., Kiss, G., Hoffer, A., Moerman, M., Henzing, B., Brinkenberg, M., Kouvarakis, G.N., Bougiatioti, K., O'Dowd, C., Ceburnis, D., Arneth, A., Svenningsson, B., Swietlicki, E., Tarozzi, L., Decesari, S., Sonntag, A., Birmili, W., Wiedensohler, A., Boulon, J., Sellegri, K., Laj, P., Baltensperger, U., Laaksonen, A., Joutsensaari, J., Petäjä, T., Kerminen, V.-M., and Kulmala M.: EUCAARI ion spectrometer measurements at 12 European sites – analysis of new particle formation events, Atmos. Chem. Phys., 10, 7907-7927, 2010.

Mihalopoulos, N., Stephanou, E., Kanakidou, M., Pilitsidis, S., and Bousquet, P.: Tropospheric aerosol ionic composition in the eastern Mediterranean region, Tellus Series B - Chemical and Physical Meteorology, 49, 314– 326, 1997.

Mirme, A., Tamm, E., Mordas, G., Vana, M., Uin, J., Mirme, S., Bernotas, T., Laakso, L., Hirsikko, A. and M. Kulmala: A wide-range multi-channel Air Ion Spectrometer, Boreal Environ. Res., 12, 247–264, 2007.

Mogensen, D., Gierens, R., Crowley, J. N., Keronen, P., Smolander, S., Sogachev, A., Nölscher, A. C., Zhou, L., Kulmala, M., Tang, M. J., Williams, J., and Boy, M.: Simulations of atmospheric OH, O_3 and NO_3 reactivities within and above the boreal forest, Atmos. Chem. Phys., 15, 3909-3932, https://doi.org/10.5194/acp-15-3909-2015, 2015.

Myriokefalitakis,S., Vignati, E., Tsigaridis, K., Papadimas, C., Sciare, J., Mihalopoulos, N., Facchini, M. C., Rinaldi, M., Dentener, F. J., Ceburnis, D., Hatzianastasiou, N., O'Dowd, C.D., van Weele, M., and Kanakidou, M.: Global modelling of the oceanic source of organic aerosols, Advances in Meteorology, doi:10.1155/2010/939171, 2010.

Myriokefalitakis S., Daskalakis, N., Fanourgakis, G. S., Voulgarakis, A., Krol, M. C., Aan de Brugh, J. M. J., and Kanakidou, M.: Pollution over the Mediterranean Basin: The Importance of Long-Range Transport on ozone and carbon monoxide, Science of The Total Environment,563–564, 40, 2016.

Nieminen, T., Asmi, A., Dal Maso, M., Aalto, P. P., Keronen, P., Petäjä, T., Kulmala, M., and Kerminen, V.-M.: Trends in atmospheric new-particle formation: 16 years of observations in a boreal-forest environment, Boreal Env. Res., 19, 191-214, 2014

O'Dowd, C. D., Hämeri, K., Mäkelä, J. M., Pirjola, L., Kulmala, M., Jennings, S. G., Berresheim, H., Hansson, H.-C., de Leeuw, G., Kunz, G. J., Allen, A. G., Hewitt, C. N., Jackson, A., Viisanen, Y., and Hoffmann, T.: A dedicated study of New Particle Formation and Fate in the Coastal Environment (PARFORCE): Overview of objectives and achievements, J. Geophys. Res., 107, 8108, doi:10.1029/2001jd000555, 2002.

Paraskevopoulou, D., Liakakou, E., Gerasopoulos, E., and Mihalopoulos, N.: Sources of atmospheric aerosol from long-term measurements (5 years) of chemical composition in Athens, Greece. Science of The Total Environment, 527–528, 165–178. http://doi.org/10.1016/J.SCITOTENV.2015.04.022, 2015.

Petäjä, T., Kerminen, V.-M., Dal Maso, M., Junninen, H., Koponen, I.K., Hussein, T., Aalto, P.P., Andronopoulos, S., Robin, D., Hämeri, K., Bartzis, J.G. and Kulmala, M.: Sub-micron atmospheric aerosols in the surroundings of Marseille and Athens: physical characterization

and new particle formation, Atmos. Chem. Phys., 7, pp. 2705-2720, doi:10.5194/acp-7-2705-2007, 2007.

Pikridas, M., Riipinen, I., Hildebrandt, L., Kostenidou, E., Manninen, H., Mihalopoulos, N., Kalivitis, N., Burkhart, J., Stohl, A., Kulmala, M. and Pandis, S. N.: NPF at a remote site in the eastern Mediterranean, J. Geophys. Res., 117, D12205, doi:10.1029/2012JD017570, 2012.

Sciare, J., Bardouki, H., Moulin, C., and Mihalopoulos, N.: Aerosol sources and their contribution to the chemical composition of aerosols in the eastern Mediterranean Sea during summertime, Atmos. Chem. Phys., 3, 291-302, https://doi.org/10.5194/acp-3-291-2003, 2003.

Salimi, F., Rahman, M. M., Clifford, S., Ristovski, Z., and Morawska, L.: Nocturnal new particle formation events in urban environments. Atmos. Chem. Phys., 17, 521–530. http://doi.org/10.5194/acp-17-521-2017, 2017.

Siakavaras, D., Samara, C., Petrakakis, M., and Biskos, G.: Nucleation events at a coastal city during the warm period: Kerbside versus urban background measurements. Atmospheric Environment, 140, 60–68. http://doi.org/10.1016/j.atmosenv.2016.05.054, 2016.

Spracklen, D. V., Carslaw, K. S., Kulmala, M., Kerminen, V.-M., Mann, G. W., and Sihto, S.-L.: The contribution of boundary layer nucleation events to total particle concentrations on regional and global scales, Atmos. Chem. Phys., 6, 5631-5648, doi:10.5194/acp-6-5631-2006, 2006.

Tammet, H., Komsaare, K., and Hõrrak, U.: Intermediate ions in the atmosphere, Atmospheric Research,135–136, 263–273,http://doi.org/https://doi.org/10.1016/j.atmosres.2012.09.009, 2014.

Tröstl, J., Chuang, W. K., Gordon, H., Heinritzi, M., Yan, C., Molteni, U., Ahlm, L., Frege, C., Bianchi, F., Wagner, R. and Simon, M., Lehtipalo, K., Williamson, C., Craven, J. S., Duplissy, J., Adamov, A., Almeida, J., Bernhammer, A.-K., Breitenlechner, M., Brilke, S., Dias, A., Ehrhart, S., Flagan, R. C., Franchin, A., Fuchs, C., Guida, R., Gysel, M., Hansel, A., Hoyle, C. R., Jokinen, T., Junninen, H., Kangasluoma, J., Keskinen, H., Kim, J., Krapf, M., Kürten, A., Laaksonen, A., Lawler, M., Leiminger, M., Mathot, S., Möhler, O., Nieminen, T., Onnela, A., Petäjä, T., Piel, F. M., Miettinen, P., Rissanen, M. P., Rondo, L., Sarnela, N., Schobesberger, S., Sengupta, K., Sipilä, M., Smith, J. N., Steiner, G., Tomè, A., Virtanen, A., Wagner, A. C., Weingartner, E.,

1 Wimmer, D., Winkler, P. M., Ye, P., Carslaw, K. S., Curtius, J., Dommen, J., Kirkby, J., Kulmala,
2 M., Riipinen, I., Worsnop, D. R., Donahue, N. M., and Baltensperger, U.: The role of low-
3 volatility organic compounds in initial particle growth in the atmosphere, Nature, 533, 527–
4 531, 2016.

5 Tzitzikalaki, E., Kalivitis, N., Kouvarakis, G., Daskalakis, N., Kerminen, V.-M., Mihalopoulos, N.,
6 Boy, M., and Kanakidou, M.: Simulations of New Particle Formation and Growth Processes at
7 eastern Mediterranean, with the MALTE-Box Model, in: Perspectives on Atmospheric
8 Sciences. T. Karacostas, A. Bais, & P. T. Nastos (Eds.), (pp. 933–939). Cham: Springer
9 International Publishing, 2017.

10 Wang, Z., Wu, Z., Yue, D., Shang, D., Guo, S., Sun, J., Ding, A., Wang, L., Jiang, J., Guo, H., Gao,
11 J., Cheung, H. C., Morawska, L., Keywood, M., and Hu, M.: New particle formation in China:
12 Current knowledge and further directions, Sci. Total Environ., 577, 258-266,
13 http://dx.doi.org/10.1016/j.scitotenv.2016.10.177, 2017.

14 Wiedensohler, A., Birmili, W., Nowak, A., Sonntag, A., Weinhold, K., Merkel, M., Wehner, B.,
15 Tuch, T., Pfeifer, S., Fiebig, M., Fjäraa, A. M., Asmi, E., Sellegri, K., Depuy, R., Venzac, H., Villani,
16 P., Laj, P., Aalto, P., Ogren, J. A., Swietlicki, E., Williams, P., Roldin, P., Quincey, P., Hüglin, C.,
17 Fierz-Schmidhauser, R., Gysel, M., Weingartner, E., Riccobono, F., Santos, S., Grüning, C.,
18 Faloon, K., Beddows, D., Harrison, R., Monahan, C., Jennings, S. G., O'Dowd, C. D., Marinoni,
19 A., Horn, H.-G., Keck, L., Jiang, J., Scheckman, J., McMurry, P. H., Deng, Z., Zhao, C. S.,
20 Moerman, M., Henzing, B., de Leeuw, G., Löschau, G., and Bastian, S.: Mobility particle size
21 spectrometers: harmonization of technical standards and data structure to facilitate high
22 quality long-term observations of atmospheric particle number size distributions, Atmos.
23 Meas. Tech., 5, 657-685, doi:10.5194/amt-5-657-2012, 2012.

24 Yli-Juuti, T., Riipinen, N., Aalto, P.P., Nieminen, T., Maenhaut, W., Janssens, I.A., Claeys, M.,
25 Salma, I., Ocskay, R., Hoffer, A., Lmre, K. and Kulmala, M.: Characteristics of new particle
26 formation events and cluster ions at K-puszta, Hungary, Boreal Environment Research, vol. 14,
27 no. 4, pp. 683-698, 2009

1 8) Tables

Day classification	Number of events	%
Total events	837	27.4
Class I	232	7.6
Class II	605	19.8
Undefined	687	22.5
Non-event	1533	50.1
Total days	3057	100.00

3 Table 1. Total available measurement days and percentage of NPF events observed at

4 Finokalia during the period June 2008-June 2018

	J_9 (cm^{-3} s^{-1})			GR_{9-25} (nm hr^{-1})			CS x 10^{-3} (s^{-1})		
	Mean	Median	SD	Mean	Median	SD	Mean	Median	SD
Winter	0.9	0.6	1.4	3.3	2.6	2.4	4.3	3.5	2.9
Spring	1.0	0.6	1.0	4.2	3.3	3.1	5.8	5.5	3.0
Summer	0.7	0.5	0.9	7.3	6.8	3.9	9.1	9.0	3.1
Autumn	0.8	0.4	1.0	5.3	4.7	2.9	6.5	6.0	3.4

6 Table 2. Formation rates for 9-nm particles (J_9), growth rates in the size range 9-25 nm (GR_{9-}

7 $_{25}$) for NPF events observed at Finokalia and condensational sink for sulfuric acid (CS) on a

8 seasonal basis during the period June 2008-June 2018 (mean, median and standard deviation).

1   9) Figures

a)   b)
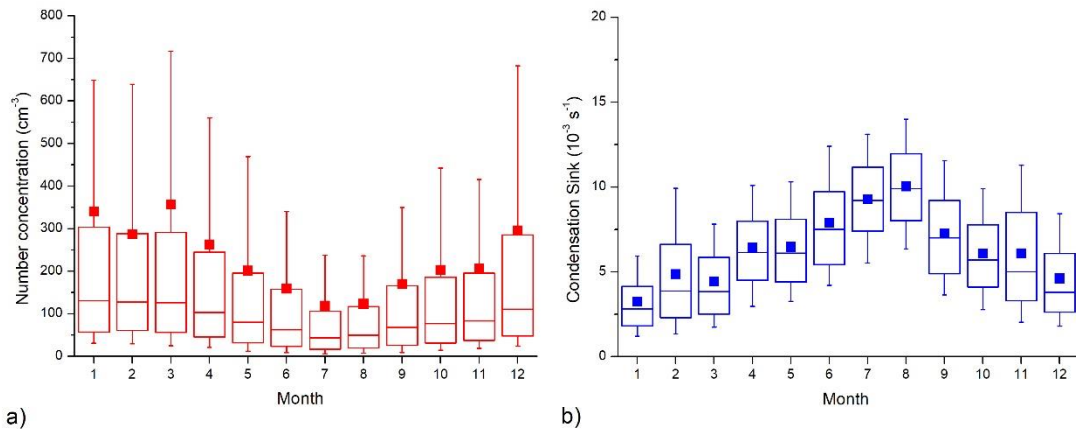
3   1. Monthly average variation of (a) nucleation mode particle number concentration and (b)

4   sulfuric acid condensational sink (*CS*) at Finokalia station over the period June 2008-June 2018.

5   Whiskers represent 10th and 90th percentiles, box edges are 75th and 25th percentiles, the

6   line in the box is the median, the solid square is the mean.

a)

b)
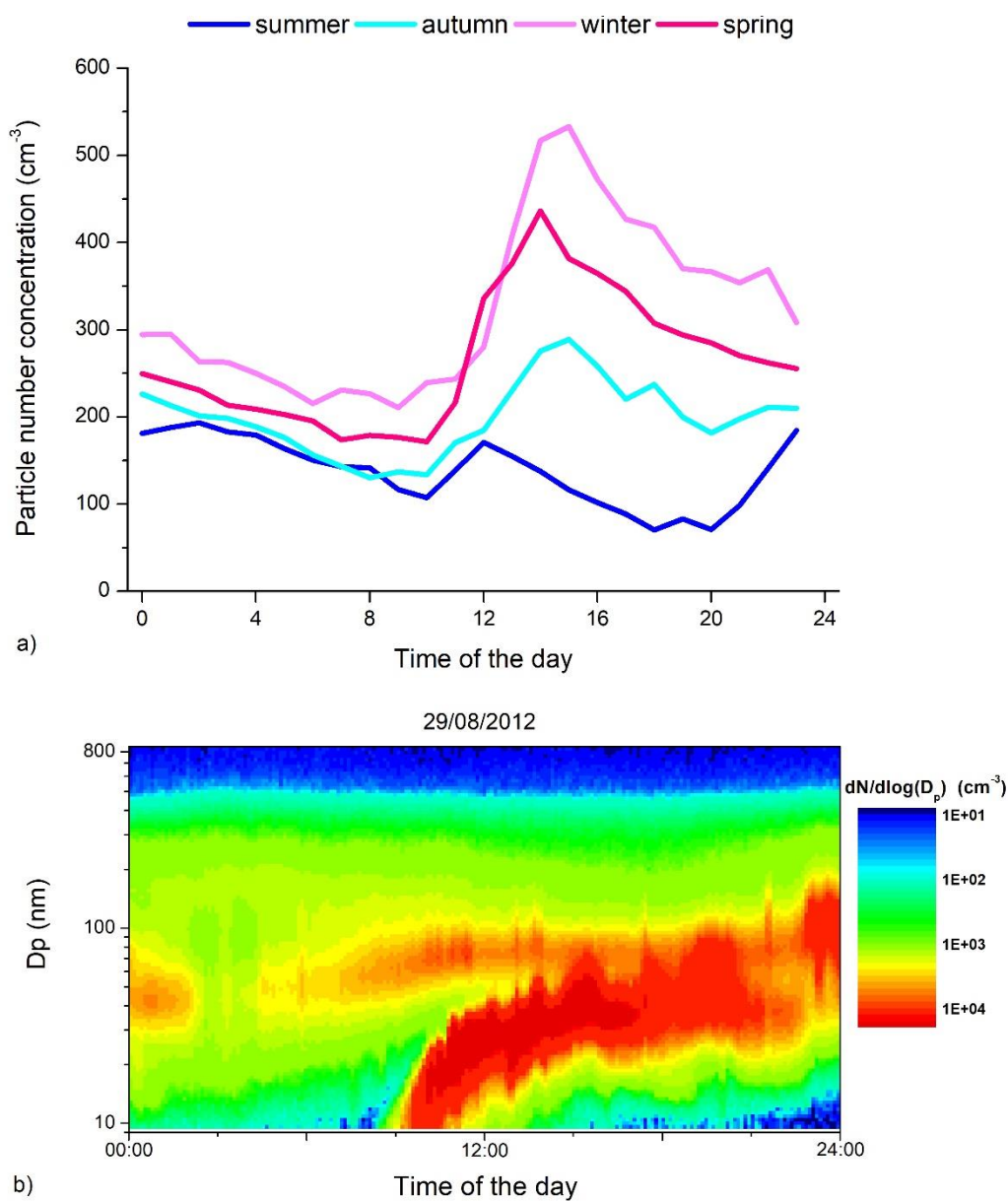
3   2. (a) Average diurnal variation of nucleation mode particle number concentration (hourly

4   values) at Finokalia over the period June 2008-June 2018. (b) New particle formation event

5   captured at Finokalia on 29/08/2012 (time in UTC+2).
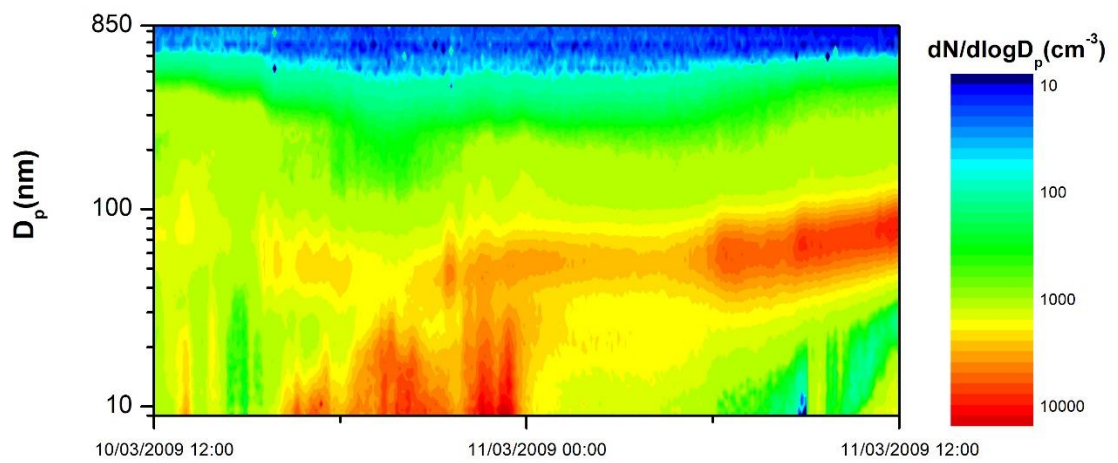
2 3. Example of appearance of nucleation mode particles during several hours as observed

3 during the night of 10 to 11/03/2009 (time in UTC+2).
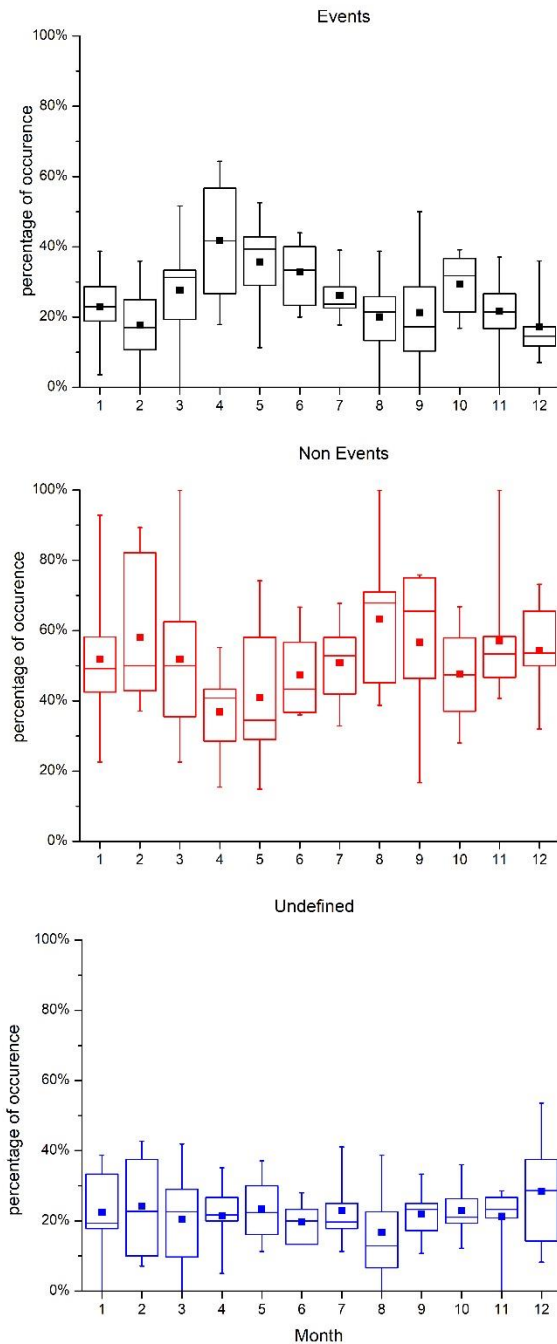
2   4. Seasonal variation of NPF percentage of occurrence of event, non-event and undefined days

3   relatively to available measurement days at Finokalia for the period June 2008-June2018.

4   Whiskers represent 10th and 90th percentiles, box edges are 75th and 25th percentiles, the

5   horizontal line in the box is the median, square is mean.
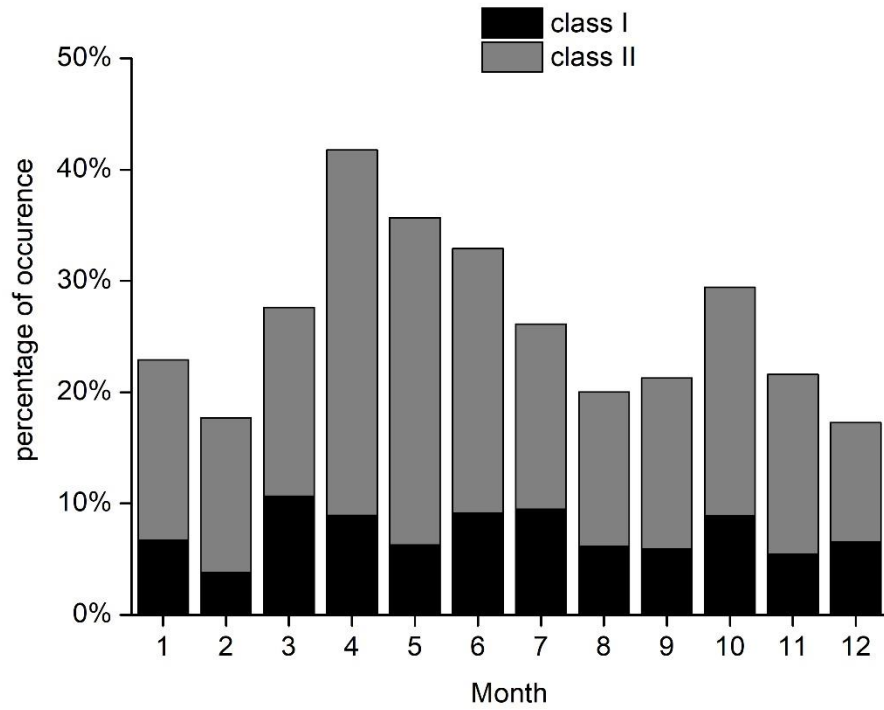
2   5. Seasonal variation of percentage of occurrence of NPF Class I & II events relatively to

3   available measurement days at Finokalia in the eastern Mediterranean for the period June

4   2008-June2018.
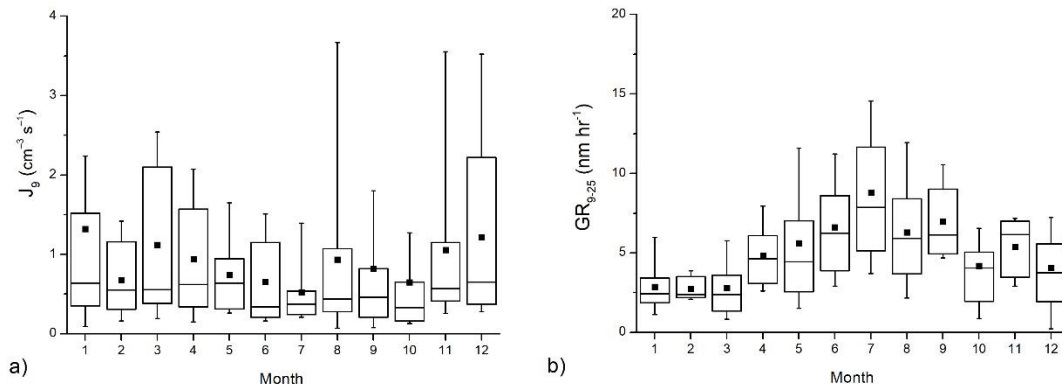
4   6. Seasonal variation of (a) formation rate of 9-nm particles (J_9) and (b) growth rate in the size

5   range 9-25nm (GR_{9-25}) as calculated during Class I NPF events at Finokalia for the period June

6   2008-June 2018. Whiskers represent 10th and 90th percentiles, box edges are 75th and 25th

7   percentiles, the horizontal line in the box is the median and the solid square is the mean.
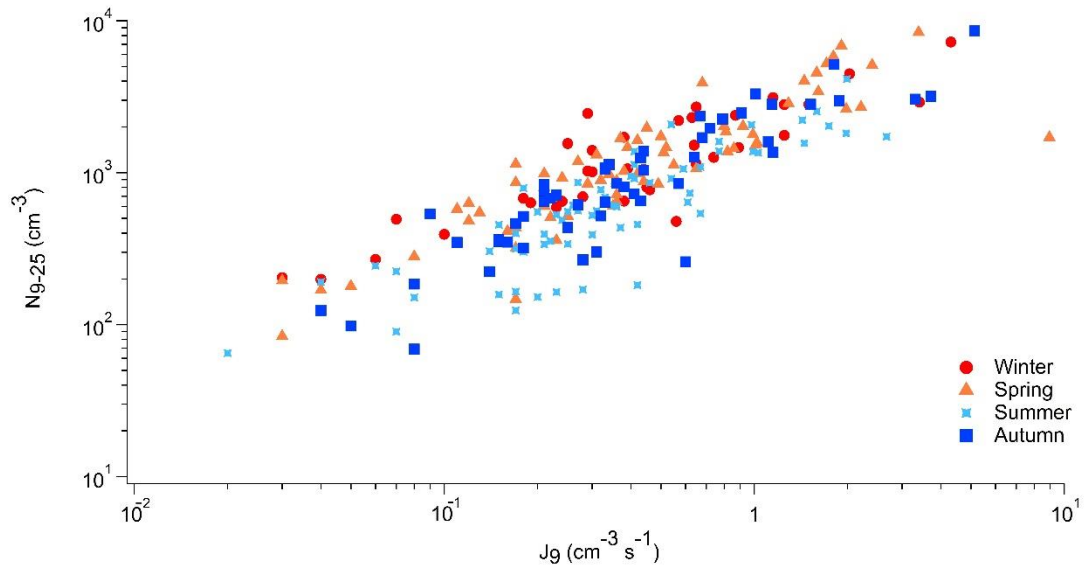
2   7. Scatter plot of the number concentration of nucleation mode particles (N_{9-25}) (hourly

3   maximum value during the event) versus formation rates of 9-nm particles (J_9) at Finokalia,

4   for events when J_9 could be calculated with a good level of confidence (Class I events).

(a) (b)

(c) (d)
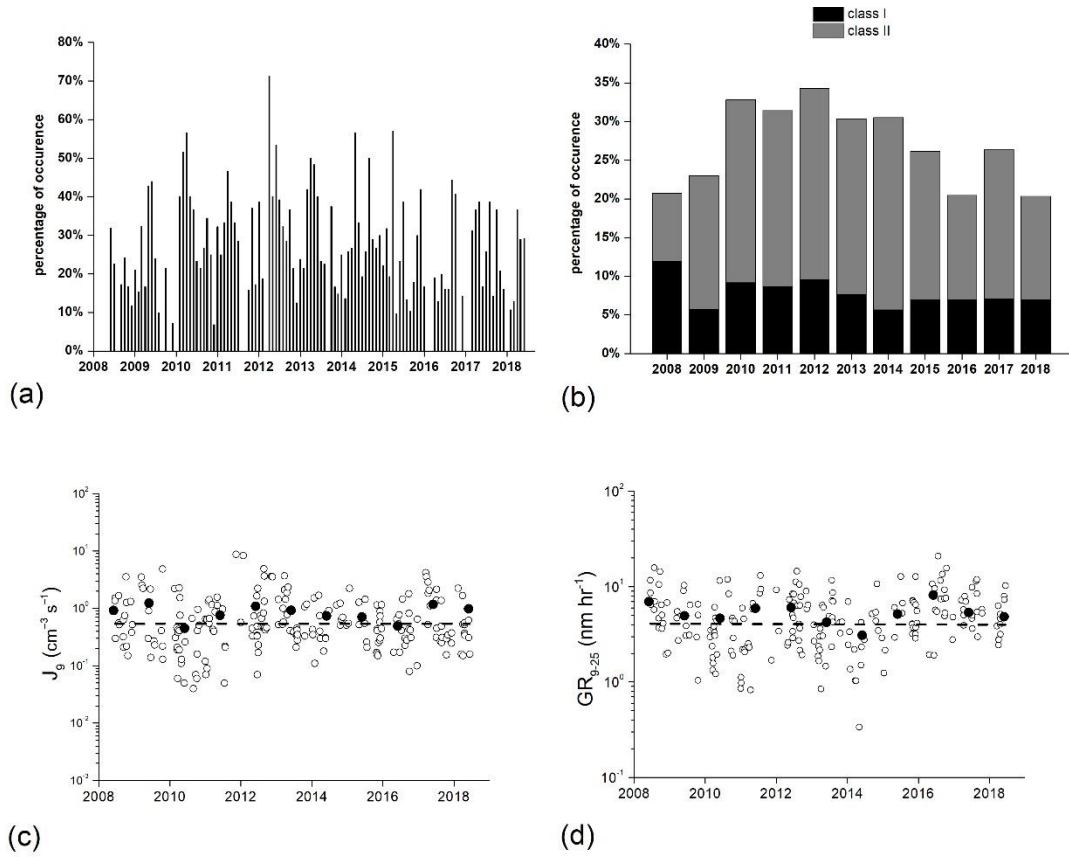
3   8. (a) Time series of monthly NPF percentage of occurrence at Finokalia for the years 2008-
4   2018. (b) Annual NPF percentage of occurrence at Finokalia for the period June 2008-June
5   2018 for Class I&II events. Interannual variation of (c) formation rates of 9-nm particles (J_9)
6   and (d) growth rate in the size range 9-25 nm (GR_{9-25}) during Class I NPF events at Finokalia for
7   the period June 2008-June 2015 (the solid circles represent annual averages and the dashed
8   lines the linear regression).
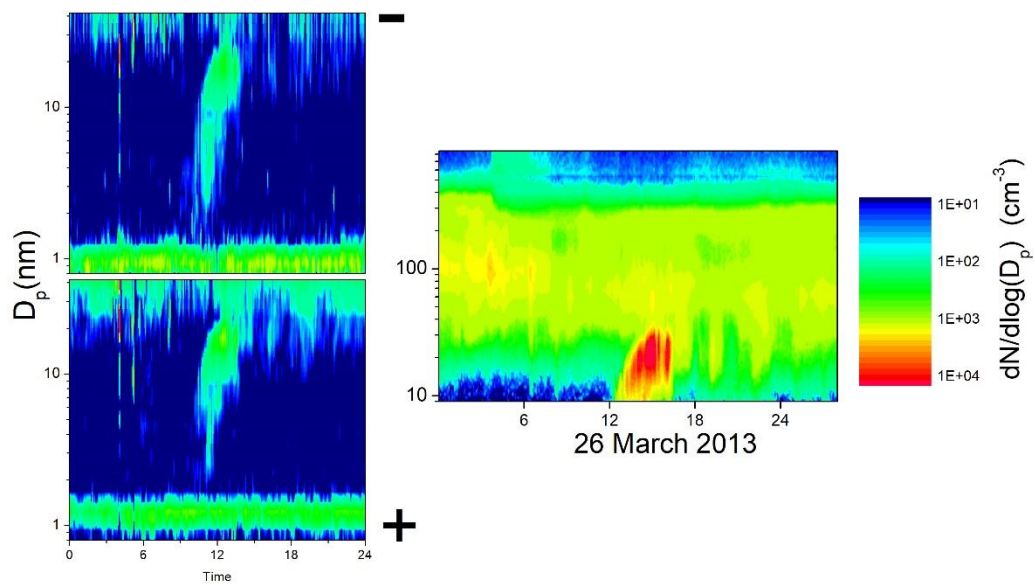
6 9. Nucleation event observed at Finokalia on 26 March 2013 as captured by AIS (left panels

7 for negative (up) and positive (bottom) polarity) and SMPS (right panel) (time in UTC+2).
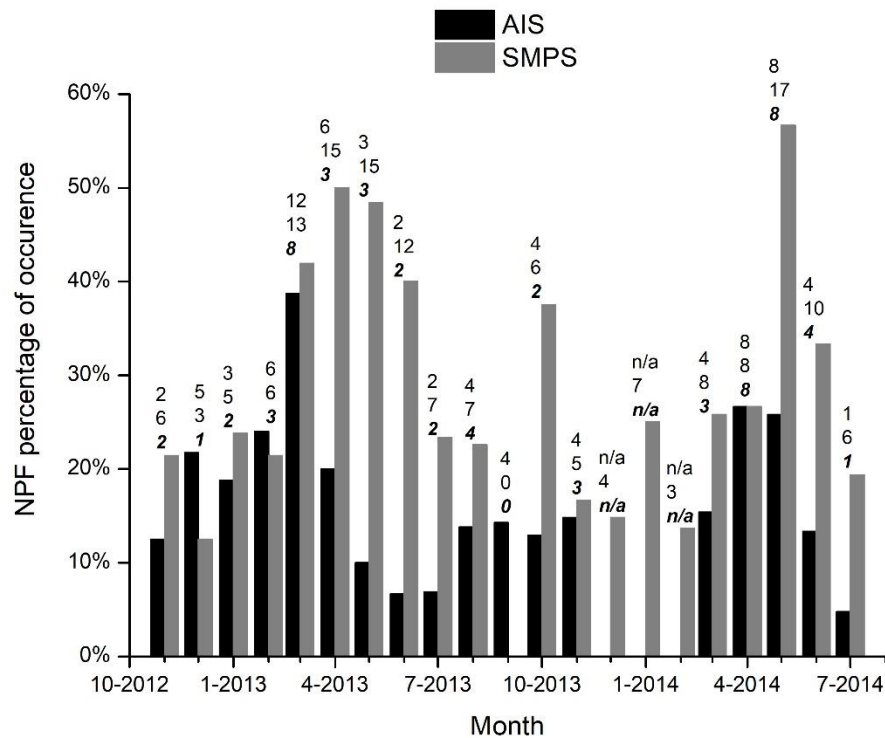
4   10. Monthly variability of NPF events' percentage of occurrence relatively to available

5   measurement days at Finokalia as determined by analysis of AIS data during the FRONT

6   experiment (Nov. 2012-July 2014). For a direct comparison, the monthly variability of NPF

7   events as obtained from the SMPS measurements for the same period is included. On top of

8   the columns, the number of NPF events observed for AIS (top), SMPS (middle) and the number

9   of common events for both instruments (bottom, italic, bold) for each month are presented.

a)

b)
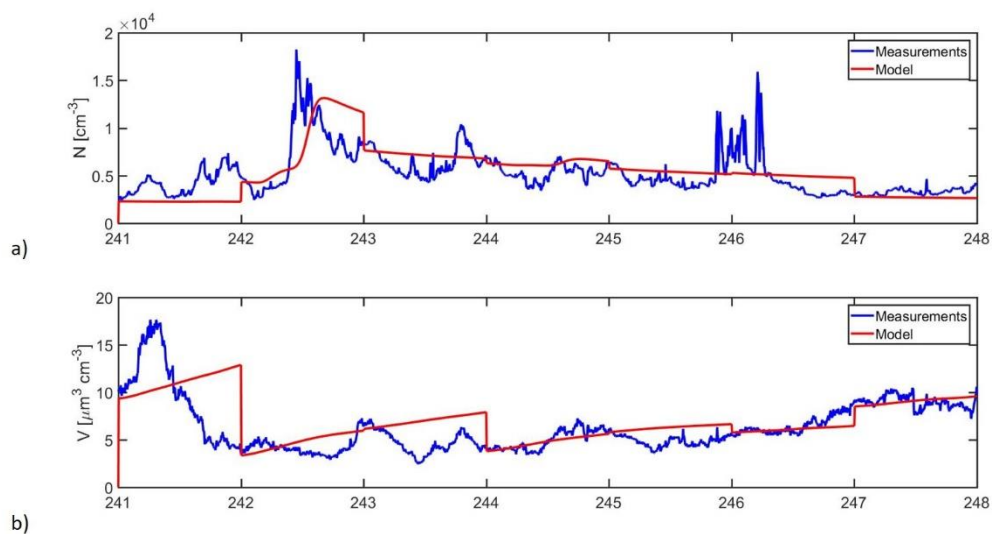
4   11. Simulations with the MALTE box with the adjusted parameters for the sub-tropical
5   environment for the "event week" that NPF events were observed at Finokalia. Measured and
6   modelled (a) total number concentration and (b) total volume concentration for the same
7   period. The x-axis in both figures is Julian day of 2012.
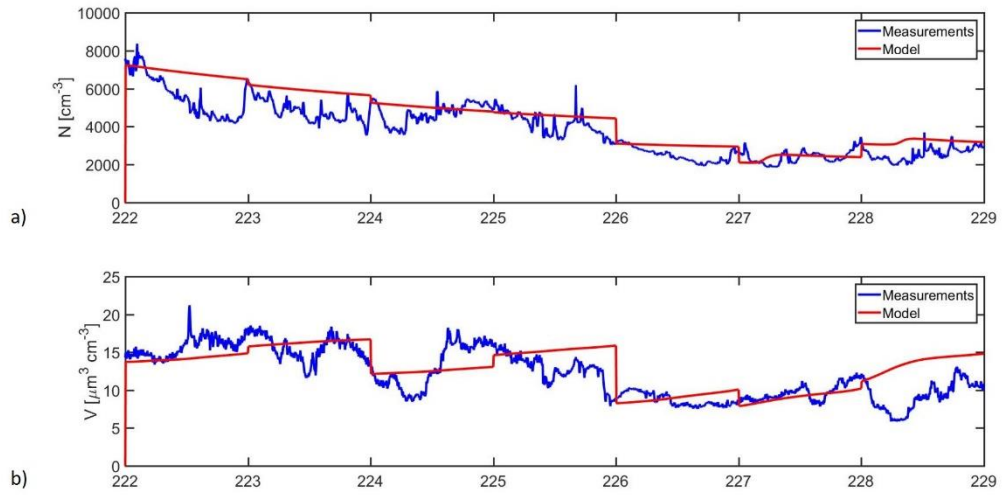
2   12. Simulations with the MALTE box with the adjusted parameters for the sub-tropical

3   environment for the "non-event" week that no NPF was observed at Finokalia. Measured

4   and modelled (a) total number concentration and (b) total volume concentration for the

5   same period. The x-axis in both figures is Julian day of 2012.